# Strong Electron-Phonon Interaction in the High-$T_c$ Superconductors: Evidence from the Infrared

Thomas Timusk
*Department of Physics, McMaster University, Hamilton, Ontario, Canada L8S 4M1*

C. D. Porter and D. B. Tanner
*Department of Physics, University of Florida, Gainesville, Florida 32611*
(Received 31 August 1990)

We show that low-frequency structure in the infrared reflectance of the high-temperature superconductor $YBa_2Cu_3O_7$ results from the electron-phonon interaction. Characteristic antiresonant line shapes are seen in the phonon region of the spectrum and the frequency-dependent scattering rate of the mid-infrared electronic continuum has peaks at 150 $cm^{-1}$ (19 meV) and at 360 $cm^{-1}$ (45 meV) in good agreement with phonon density-of-states peaks in neutron time-of-flight spectra that develop in superconducting samples. The interaction between the phonons and the charge carriers can be understood in terms of a charged-phonon model.

PACS numbers: 74.30.Gn, 72.10.Di, 74.70.Vy, 78.20.Ci

Phonons have generally been viewed as being of secondary importance in the overall properties of high-$T_c$ superconductors for four reasons. (1) The isotope shift of $T_c$ is small, especially in $YBa_2Cu_3O_7$. (2) The value of $T_c$—100 K—seems too large for phonon energies to set the scale. (3) The insulating phases show strong magnetic effects with an energy scale higher than the phonons. (4) The electrical resistivity has a nearly linear temperature dependence over a wide temperature range,[1] with a scattering rate $1/\tau \approx (1-2)k_BT$, suggesting weak electron scattering from some low-frequency excitation, below typical phonon frequencies. However, there are several observations which suggest that phonons may be more central to the problem than previously believed. Among these are the following: (1) The phonon density of states as measured by neutron time-of-flight (TOF) spectroscopy[2] shows pronounced softening as the materials are changed from insulating parent compounds to conductors and superconductors. (2) Certain phonon branches—related to Cu-O stretches—show anomalies near the zone boundary.[3] These anomalies have been attributed to a strong electron-phonon interaction. (3) There are well-known changes in Raman frequencies as well as line shapes which indicate interaction of the Raman-active modes with an underlying electronic continuum.[4] (4) There is recent evidence for a large isotope shift of $T_c$ at particular dopant concentrations in $La_{2-x}Ba_xCuO_4$ and $La_{2-x}Sr_xCuO_4$ (Ref. 5) and in $YBa_2Cu_3O_7$.[6]

The strongest evidence for an unconventional electron-phonon interaction comes from neutron-scattering results. Renker *et al.*[2] working with $YBa_2Cu_3O_7$ and Currat *et al.*[7] with $Pb_2Sr_2(Y,Ca)Cu_3O_{9-\delta}$ notice dramatic changes in TOF spectra in the copper-oxygen stretching-mode region, changes that cannot be attributed to structural differences alone. Figures 1(a) and 1(b), from Renker *et al.*, illustrate these effects. These differences are confirmed by recent inelastic neutron-scattering measurements of Reichard *et al.*[3] on $YBa_2Cu_3O_7$, which show a remarkable broad phonon branch in the same spectral region, near the zone boundary. Reichard *et al.* interpret this as evidence for strong electron-phonon coupling.

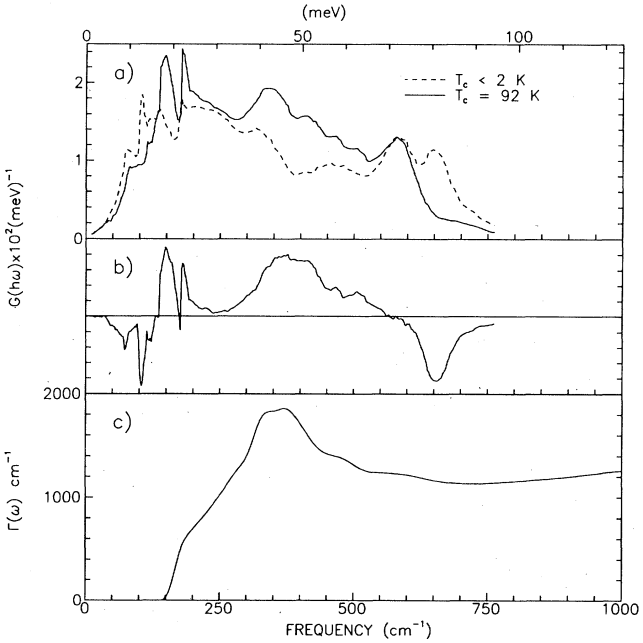


FIG. 1. (a) Neutron density of states for phonons from Renker *et al.* (Ref. 2) for $YBa_2Cu_3O_x$. The solid curve is for a superconducting sample ($x=7$) and the dashed curve is for a nonsuperconducting one ($x=6$). There is a strong enhancement of density of states in the 19- and 50-meV regions. (b) A difference spectrum between the two curves in (a). (c) The frequency-dependent scattering rate determined from the mid-infrared conductivity.

The *a-b*-plane infrared properties of the high-$T_c$ materials are those of a poor metal with no obvious phonon peaks, but they are decidedly non-Drude in nature.[8] There appear to be two components to the optical conductivity: A low-frequency free-carrier band which tracks the dc conductivity above $T_c$ and which forms the superconducting condensate at low temperature[9] and a mid-infrared band of comparable spectral weight but with a much higher width.[10,11] The mid-infrared conductivity is seen best in the superconducting state where the free carriers have condensed. In $YBa_2Cu_3O_7$ it forms a broad continuum peaking at 800 $cm^{-1}$ (100 meV) with a characteristic notchlike minimum at 420 $cm^{-1}$ (52 meV).[12-15] The notch at 420 $cm^{-1}$ does not shift in position if $T_c$ is reduced by oxygen depletion.[15] At still lower frequencies the conductivity drops, to the extent that in some samples a gaplike onset at 150 $cm^{-1}$ (19 meV) is observed. Other investigators do not find a gap but instead a region of modest but finite conductivity at low frequency.[16] Even so, there is *some* structure in the conductivity in the 150-$cm^{-1}$ (19-meV) region. In many spectra both features can be seen above the superconducting transition; in some cases up to room temperature.[14,15] In light of the inertness of these features to changes in doping level and superconducting state, it is most natural to attribute both features to phonons rather than electronic effects.

In this paper we present evidence for this view. We show that the conspicuous structure in the infrared absorption of the oxide superconductors can be understood in terms of linear coupling between certain phonons and the charge carriers responsible for the mid-infrared absorption. This interaction differs from a Holstein sideband, a characteristic manifestation of the electron-phonon interaction in ordinary metals. In the Holstein phonon-emission process, each new phonon branch gives rise to a step or threshold in the scattering rate $\Gamma(\omega)$. In the mechanism described in this paper, the *electronic* scattering rate $\Gamma(\omega)$ is directly proportional to the density of states of the *phonons* that interact most strongly with the charge carriers. Such processes are not new. They occur in organic conductors, where charge-density waves can give internal molecular vibrations electronic-strength infrared intensities.[17]

To find $\Gamma(\omega)$ we make the assumption that seems to give the best description of the optical conductivity spectra,[14] namely, that the dielectric function is made up of three parallel channels, a free-carrier part $\epsilon_D$, a mid-infrared electronic part $\epsilon_e$, and a high-frequency contribution $\epsilon_\infty$:

$$\epsilon(\omega)=\epsilon_D+\epsilon_e+\epsilon_\infty . \tag{1}$$

We write $\epsilon_e$ in terms of the frequency-dependent scattering rate[18,19]

$$\epsilon_e=\frac{\omega_{pe}^2}{\omega I(\omega)-\omega^2-i\omega\Gamma(\omega)} , \tag{2}$$

where $\omega_{pe}$ is the plasma frequency of the mid-infrared band and $\Gamma(\omega)$ and $I(\omega)$ describe the real and imaginary parts of the frequency-dependent scattering rate. In the superconducting state, in the clean limit, the free-carrier portion of the conductivity collapses to a $\delta$ function at the origin, leaving zero oscillator strength at finite frequencies. With $\epsilon_e=\epsilon_{e1}+i\epsilon_{e2}$, we can get $\epsilon_{e2}$ by Kramers-Kronig analysis from reflectance experiments and $\epsilon_{e1}$ from a second Kramers-Kronig transformation of $\epsilon_{e2}$. Thus, the frequency-dependent scattering rate,

$$\Gamma(\omega)=\omega_{pe}^2\epsilon_{e2}/\omega(\epsilon_{e1}^2+\epsilon_{e2}^2) , \tag{3}$$

can be obtained *directly* from the experimentally determined $\epsilon(\omega)$ at low temperature. Apart from the oscillator strength of the mid-infrared band $\omega_{pe}$ (taken from Kamarás *et al.*[14]), which sets the overall scale of $\Gamma(\omega)$, this procedure to determine the frequency-dependent scattering rate involves no fitted parameters.

Figure 1(c) shows $\Gamma(\omega)$ obtained from the low-temperature conductivity spectra of Kamarás *et al.* for a laser-ablated film of $YBa_2Cu_3O_7$. The spectrum has an onset in the 150-$cm^{-1}$ (19-meV) region, a broad peak centered at 360 $cm^{-1}$ (45 meV), followed by a fairly constant scattering rate of the order of 1000 $cm^{-1}$, due to the inelastic processes of the mid-infrared absorption. We will focus on the structure in the phonon region, 100–700 $cm^{-1}$.

The most conspicuous feature of $\Gamma(\omega)$ is the broad peak in the center of the phonon band at 360 $cm^{-1}$ (45 meV). Its center frequency is in good agreement with the center of the neutron TOF peak in the difference spectrum of Renker *et al.* shown in Fig. 1(b). The strength of the band can also be expressed as a contribution to $\lambda$ through the approximation $\lambda\approx\pi\Gamma(\omega_0)d\Gamma/2\omega^2$, where $d\Gamma$ is the width of the peak in $\Gamma(\omega_0)$ and $\omega_0$ its center frequency. With $\Gamma(\omega_0)=1900$ $cm^{-1}$, $\lambda\approx 2.9$ is found for the 360-$cm^{-1}$ band.

The onset of scattering in the 150-$cm^{-1}$ (19-meV) region in Fig. 1(c) is a reflection of the gaplike depression in conductivity below this frequency in the spectra of Kamarás *et al.* Other results, for example the recent bolometric measurements of absorption of Pham *et al.*,[16] show a more gradual $\omega^2$ dependence of absorption at low frequency. Apart from experimental difficulties of accurate measurements of low absorption levels of 0.5% and less, the variation in this spectral region appears to be sample dependent. Nevertheless, one can identify, in all the high-quality spectra, a feature at 150 $cm^{-1}$ (19 meV).

The trick of calculating $\epsilon_{1e}$ by Kramers-Kronig analysis of $\epsilon_{2e}$ only works below $T_c$. At and above $T_c$, the free-carrier part of the dielectric function begins to enter the picture. To look at the temperature dependence we use a model with three broad oscillators to describe the optical response.[20] The parameters of the broad oscillators are fitted to give good overall agree-

ment with the reflectance curves. Such a model fails to give the characteristic "knees" seen in the reflectance spectra [Fig. 2(b), long-dashed curves]. We therefore introduce a frequency-dependent damping of $\Gamma(\omega)=\gamma_e+C\Delta G(\omega)$, where $\Delta G(\omega)$ is based on the neutron TOF difference spectrum of Fig. 1(b). The overall coupling strength $C$ to the phonons is adjusted to give a peak at the center of the 375-cm$^{-1}$ band of Renker *et al.*[2] of $\Gamma=400$ cm$^{-1}$ in the normal state and $\Gamma=1900$ cm$^{-1}$ in the superconducting state. This increase in the strength of the electron-phonon coupling as $T$ is lowered is seen in experimental spectra[14] as a deepening of the 420-cm$^{-1}$ notch in $\sigma_1(\omega)$.

The free-carrier contribution $\epsilon_D$ is represented by a Drude-model dielectric function, with oscillator strength and linewidth from Kamarás *et al.*[14] These parameters are in accord with the dc conductivity. (We note that the $T$ dependence of $\sigma_{dc}$ necessarily implies a corresponding frequency dependence to $1/\tau$. However, the linear $T$ dependence of $1/\tau$ mentioned above implies a relatively weak scattering of the charge carriers by low-energy excitations, with $\lambda_T\sim 0.3$. In turn, this leads to only modest deviations from the Drude formula at the lowest frequencies. Therefore, we feel justified in our use of the Drude model for the free-carrier contribution to the dielectric function.)

Using this simple model, we calculate the reflectance spectra shown in Fig. 2(b). The experimental spectra[14] are shown in Fig. 2(a). There is good qualitative agreement between the measured spectra and the calculated

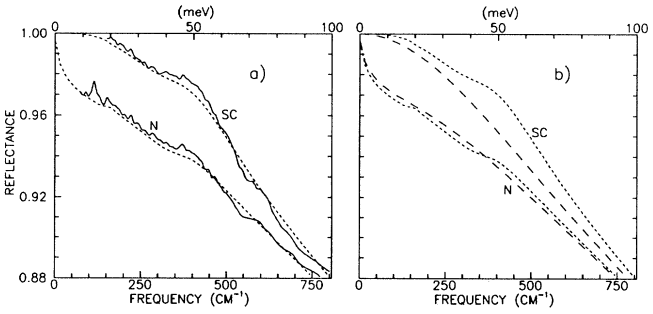


FIG. 2. (a) Reflectance of an $a$-$b$-plane–oriented film with $T_c=89$ K of $YBa_2Cu_3O_{7-\delta}$ according to Kamarás *et al.* (Ref. 14) at 20 K (upper solid curve) and 100 K (lower). The short-dashed curves are a model calculation of the infrared reflectance with a simple two-component dielectric function. The first component represents the free carriers and is assumed to take on zero width in the superconducting state. The second component is a Drude term, with the charge carriers coupled to phonons. The frequency dependence of the coupling is taken from the neutron measurements in Fig. 1(b). (b) The short-dashed curves are the electron-phonon calculation also shown in (a). The long-dashed curves are calculations without coupling to the phonons. The phonon peaks account for the two knees seen in many reflectance spectra at 150 and 420 cm$^{-1}$.

ones. The important point of Fig. 2 is that the sharp features—the knee at 420 cm$^{-1}$ and the onset at 150 cm$^{-1}$—originate from the phonon density of states and not the model parameters. This is clear from the long-dashed curves of Fig. 2(b), where the electron-phonon coupling strength is set to zero and these features are absent.

It can be seen from Fig. 2 that the model with the TOF spectrum as input describes the two-kneed shape of the infrared reflectance spectrum well for both the superconducting and the normal states. Note the appearance of a weak *peak* in the normal state at the position of the 19-meV phonon. The experimental spectra in the normal state generally show a weak peak at this frequency, a characteristic of reflectance spectra of excitations that enter as peaks in $\Gamma(\omega)$. A phonon that is directly coupled to the electromagnetic field gives rise to a *minimum* in the reflectance spectrum. (The opposite relation holds in the conductivity spectrum.) In the superconducting state (assumed to be described by a clean-limit London model), this sharp peak, if strong enough, develops into a threshold for absorption.

Peaks in $\Gamma(\omega)$ at phonon frequencies and notchlike antiresonances in the conductivity are commonly seen in spectra of organic conductors. They arise from a Fano-like interference between an electronic continuum and discrete, totally symmetric phonons.[21,22] Called the "charged-phonon" mechanism by Rice, the process gives normally forbidden phonons oscillator strengths of electronic magnitude, much larger than directly coupled optic phonons.[23] We suggest that the phonon structure seen in the high-$T_c$ superconductors arises from such a mechanism.

In the organic conductors, charge-density waves supply the symmetry-breaking potential that couples the electromagnetic radiation to modes that are not at $q=0$. In the case of the high-$T_c$ oxides, a potential will also be needed to allow IR activity of the zone-boundary modes seen by neutron spectroscopy to couple strongly to the electrons. We do not know the source of this potential, but in view of the universality of the 420-cm$^{-1}$ knee in reflectance spectra and because the coupling gets stronger as the temperature is lowered[14] some intrinsic process such as an incipient structural instability may be responsible. The high degree of variability of the 150-cm$^{-1}$ mode coupling suggests that its activation may be associated with defects.

The measurements of Kamarás *et al.*[14] that we have analyzed here were made on twinned films and thus represent a superposition of $a$- and $b$-axis conductivities. There is evidence that the chains in the $YBa_2Cu_3O_7$ structure make a separate contribution to the conductivity in the form of a broad peak centered at 0.5 eV.[10,24,25] We have used a broad Lorentzian for this band in the calculations shown in Fig. 2. In principle, we should introduce a fourth channel of conductivity to account for

any transport on the chains and subtract this contribution before proceeding to analyze the *a-b*-plane properties. This is difficult since the *a-b* plane itself may be quite anisotropic. That the anisotropy is substantial is clear from the Raman scattering work of Slakey *et al.*[4] on untwinned crystals. Both the electronic Raman scattering and the coupling between the phonons and the background continuum at 116 $cm^{-1}$ are stronger in the chain direction than normal to the chain. The electronic Raman scattering shows that both the continuum and the Fano-type coupling to the phonons is present in both directions in the *a-b* plane.

The present analysis can be extended to other high-$T_c$ superconductors where there are neutron TOF spectra available in superconducting and nonsuperconducting varieties of the same structure. Infrared spectra of $Bi_2Sr_2CaCu_2O_8$,[26] $Tl_2Ba_2CaCu_2O_8$,[27] and $Pb_2Sr_2(Y, Ca)Cu_3O_{9-\delta}$ (Ref. 28) all show features similar to those in $YBa_2Cu_3O_{7-\delta}$. A detailed study of these phonon features may lead to an understanding of the transitions that are responsible for the mid-infrared band.

We have shown that properties of the widely reported and puzzling infrared features, the knee at 420 $cm^{-1}$ and the feature at 150 $cm^{-1}$, can be understood within a model of charged phonons, coupled to the mid-infrared electronic transition. The model accounts for the remarkable insensitivity of these features to changes in doping level and the superconducting transition. The frequency-dependent scattering rate of this process mirrors the changes in the neutron density of states of phonons associated with superconductivity.

The identification of the processes that lead to the structures in the far-infrared spectra as charged-phonon processes of the type first studied by Rice in organic crystals has a more fundamental significance than clearing up the puzzle and controversy about the structures in the optical conductivity that have been assigned to the superconducting gap.[12,13,29] The strong coupling of the electrons responsible for the mid-infrared absorption to certain phonons may be relevant to the electronic mechanism of superconductivity.

We thank J. P. Carbotte, H. D. Drew, C. Kallin, M. Reedyk, and M. J. Rice for valuable discussions. The research at McMaster University is supported by the Natural Sciences and Engineering Research Council of Canada (NSERC) and the Canadian Institute for Advanced Research (CIAR). Work at University of Florida is supported by U.S. Defense Advanced Research Projects Agency through Contract No. MDA972-88-J-1006.

[1]M. Gurvitch and A. T. Fiory, Phys. Rev. Lett. **59**, 1337 (1987).
[2]B. Renker *et al.*, Z. Phys. B **73**, 309 (1988).
[3]W. Reichard *et al.*, Physica (Amsterdam) **162–164C**, 464 (1989).
[4]F. Slakey *et al.*, Phys. Rev. B **39**, 2781 (1989).
[5]M. F. Crawford *et al.*, Phys. Rev. B **41**, 282 (1990).
[6]J. P. Franck *et al.* (unpublished).
[7]R. Currat *et al.*, Phys. Rev. B **40**, 11362 (1989).
[8]K. Kamarás *et al.*, Phys. Rev. Lett. **60**, 969 (1988).
[9]D. A. Bonn *et al.*, Phys. Rev. B **37**, 1547 (1988).
[10]K. Kamarás *et al.*, Phys. Rev. Lett. **59**, 919 (1987).
[11]T. Timusk *et al.*, Phys. Rev. B **38**, 6683 (1988).
[12]G. A. Thomas *et al.*, Phys. Rev. Lett. **61**, 1313 (1988).
[13]J. Schützmann *et al.*, Europhys. Lett. **8**, 679 (1989).
[14]K. Kamarás *et al.*, Phys. Rev. Lett. **64**, 84 (1990).
[15]S. L. Cooper *et al.*, Phys. Rev. B **40**, 11358 (1989).
[16]T. Pham *et al.*, Phys. Rev. B **41**, 11681 (1990).
[17]M. J. Rice, Phys. Rev. Lett. **37**, 36 (1976).
[18]W. Götze and P. Wölfle, Phys. Rev. B **6** 1266 (1972).
[19]J. W. Allen and J. C. Mikkelsen, Phys. Rev. B **15**, 2952 (1977).
[20]The parameters used for the 100-K calculations (in $cm^{-1}$) are as follows: $\omega_{pD}=8200$, $\gamma_D=140$, $\omega_{pe}=15000$, $\gamma_e=2200$. Finally, a Lorentz oscillator, with $\omega_{pL}=7800$, $\gamma_L=15000$, and $\omega_{0L}=3300$, is used to represent the higher-frequency contribution from the chains. In the superconducting state $\gamma_D=0$; all other parameters are unchanged.
[21]M. J. Rice, V. M. Yartsev, and C. S. Jacobsen, Phys. Rev. B **21**, 3437 (1980).
[22]M. J. Rice and Y. R. Wang, Phys. Rev. B **36**, 8794 (1987).
[23]S. Tajima *et al.*, Physica (Amsterdam) **168C**, 117 (1990).
[24]J. Tanaka *et al.*, Physica (Amsterdam) **153–155C**, 1752 (1988).
[25]J. Orenstein *et al.*, Phys. Rev. B **42**, 6342 (1990).
[26]M. Reedyk *et al.*, Phys. Rev. B **38**, 11981 (1988).
[27]C. M. Foster *et al.* (unpublished).
[28]M. Reedyk *et al.*, Bull. Am. Phys. Soc. **35**, 814 (1990).
[29]R. T. Collins *et al.*, Phys. Rev. Lett. **63**, 422 (1989).